NANO LETTERS

2007
Vol. 7, No. 4
950−955

Low-Frequency Electrophoretic Actuation of Nanoscale Optoentropic Transduction Mechanisms

Benjamin David Sullivan,[†] Dietrich A. Dehlinger,[‡] Sanja Zlatanovic,[‡] Sadik A. Esener,[‡] and Michael J. Heller*[,†,‡]

Department of Bioengineering, and Department of Electrical and Computer Engineering, University of California, San Diego, 9500 Gilman Drive, La Jolla, California 92093

Received December 21, 2006; Revised Manuscript Received February 27, 2007

ABSTRACT

Inherent bistabilities within DNA-assembled fluorescent resonant energy transfer systems demonstrated time-varying optical signals in response to an electrophoretic driving force. Frequency responses of electrophoretically driven FRET systems were shown to be sequence specific. Integration of these signals over time gave near single-molecule sensitivity within a high background of autofluorescence. This research suggests that externally driven nanoscale mechanical systems may help improve information flow within morphologically intact specimens.

It has long been recognized that detection of early-stage mutations within cancer would yield insight into therapeutic approaches, yet genotyping assays remain far from the forefront of clinical practice. Data indicate that soluble mRNA from circulating metastases are expressed at levels over 10 times below the threshold for reliable RT-PCR techniques.[1,2] At such low levels, detection becomes inconsistent, forcing clinicians to examine secondary markers for the disease that only partially correlate to disease pathogenesis.[3,4]

In response to these barriers, considerable effort has been made in the past decade to develop methodologies that enable direct detection of molecular targets without PCR amplification.[5−17] For example, some of the more well-known techniques available in the literature include: (1) nanoparticle assays based on quantum dots, plasmon resonant nanoparticles (nanoshells), fluorescent polymer beads, gold nanoparticles, and immunomagnetic preciptations; (2) device-based methodologies such as quartz crystal microbalances, electrochemical detection, fiber-optic microbead arrays, nanochannels, and nanoelectrodes; (3) spectroscopic techniques including SERS, TCSPC, functionalized AFM, NSOM, MHz-TIRF, and near field approaches, microsphere whispering mode galleries; (4) biochemical techniques centered around enzyme-assisted detection, modified nucleic acids, PNA, LNA, and water-soluble conjugated polymers; (5) mechanistic approaches that employ nanoparticle aggregation or molecular beacons.

Despite the advent of individually detectable nanoparticles, single-molecule resolution has yet to translate into a viable platform for mapping the genetic changes associated with early stages of cancer progression. Sensitive assays are generally compromised when converted to complex biological samples such as tissue sections, smears, or whole blood. In particular, nanoparticle probes meant to detect DNA by hybridization regularly bind to cell matrices, proteins, and other sections of the genome.[18,19] For rare targets, this background is often the lower limit of detection.

Typically, short genetic probes are allowed to diffuse throughout a sample in order to locate and bind to a complementary DNA sequence. Passive hybridization allows oligonucleotides to repeatedly explore local free energy minima such as mismatched binding sites or nonspecific traps. In the presence of genomic DNA, these mismatched sites present kinetic- and concentration-dependent barriers to the probes finding complementary sequences.[19]

In this study, we explore a nanoscale mechanism to help distinguish background binding from specific hybridization in ensemble measurements of hybridized DNA. Early work by Heller et al., demonstrated that the ends of double-stranded oligonucleotide probes spent more time in solution than the center of the probe (Figure 1A).[20] Here, we demonstrate that low levels of electrophoretic force below the dehybridization threshold can initiate oscillatory behavior from the frayed ends of intermolecular fluorescent resonant energy transfer (FRET) constructs.

It is expected that externally driven FRET systems will provide detailed information about the instantaneous free energy of detected species. Position- and sequence-dependent

* Corresponding author. E-mail: mheller@bioeng.ucsd.edu.
[†] Department of Bioengineering.
[‡] Department of Electrical and Computer Engineering.

10.1021/nl063014x CCC: $37.00
Published on Web 03/14/2007

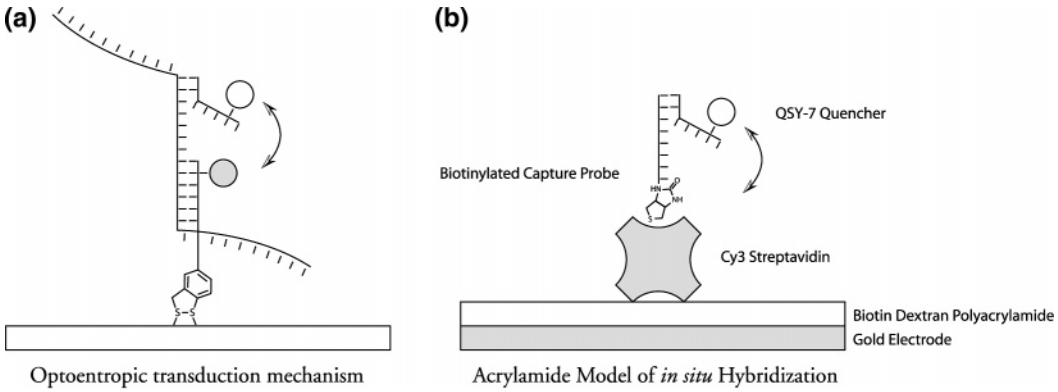

Figure 1. (A, left) Example of the proposed hinged transduction mechanism. Fluorescence from the donor (dark circle) to acceptor (light circle) is modulated by an applied driving force to convert mechanical motion into a time varying optical signal. (B, right) Model system used to explore electrophoretic actuation of surface bound FRET systems. The fluorescent amplitude of the Cy3-labeled streptavidin is modulated by the induced behavior of the QSY-7 quencher probe.

Chart 1

Complementary:	3′-QSY7-CTT-GTC-GAA-ACT-CCA-CGC-AC-5′
1 bp mismatch:	3′-QSY7-CTc-GTC-GAA-ACT-CCA-CGC-AC-5′
2 bp mismatch:	3′-QSY7-CTc-GTt-GAA-ACT-CCA-CGC-AC-5′
Noncomplementary:	3′-QSY7-CTa-cTC-Gtc-Aag-atg-CaC-c-5′

opening energetics have been observed with imino proton exchange NMR, and rehybridization of DNA hairpin molecules have been shown to be slowed by entropic traps during the postnucleation hybridization process.[21−23] Therefore the kinetics of both opening and rehybridization are likely to depend upon the complementarity of the target DNA involved in assembling the FRET system. Similar mechanisms have been used to quantify intramolecular hairpin dynamics using thermal denaturation, but these methods have not been applied to mechanisms appropriate for intermolecular modulation.[22,24] It is the purpose of the current study to explore whether low-frequency actuation of these constructs can provide a measure of differentiation from nonspecific binding.

A polyacrylamide model of in situ hybridization was used to study vertically oriented electrophoretic actuation of surface bound FRET systems (Figure 1B). Briefly, 14 μM biotin dextran [Sigma-Aldrich] was prepared in a 19:1 acrylamide:bis TBE buffer solution and cured atop gold slides within 5 mm diameter insulated wells of approximately 100 μm in height. Cy3-conjugated streptavidin (Sigma) was functionalized with a 1:1 concentration of biotinylated capture DNA from the p53 gene (5′-biotin-GAA-CAG-CTT-TGA-GGT-GCG-TGT-TTG-TGC-CTG-TCC-TGG-GAG-AGA-CCG-GCG-CAC-3′) and mixed with equimolar amounts of complementary, 1-base pair mismatched, or 2-base pair mismatched QSY-7 quencher probes (Chart 1, Figure 2). DNA was purchased from TriLink Biotechnologies, San Diego, CA.

Cy3−streptavidin FRET systems were bound to the surface of the acrylamide covered electrodes, washed in a high-salt buffer (0.5 M NaCl, 0.05 M sodium phosphate pH 7.0), and immersed in 400 μL of 0.01X TBE buffer immediately prior to electrophoretic actuation. Low-salt and low-conductivity buffers were chosen to slightly destabilize hybridization at room temperature to allow the electric field to perturb the DNA. A 32 gauge platinum counter electrode was positioned adjacent to the gel construct, followed by application of an electric field stringency protocol (−1 V to −6 V in −0.1 V/s, Keithley 237, Keithley Instruments) used to precondition the system and to select a consistent free energy threshold above which unstable probes would be actively transported away from the field of view (Figure 3).

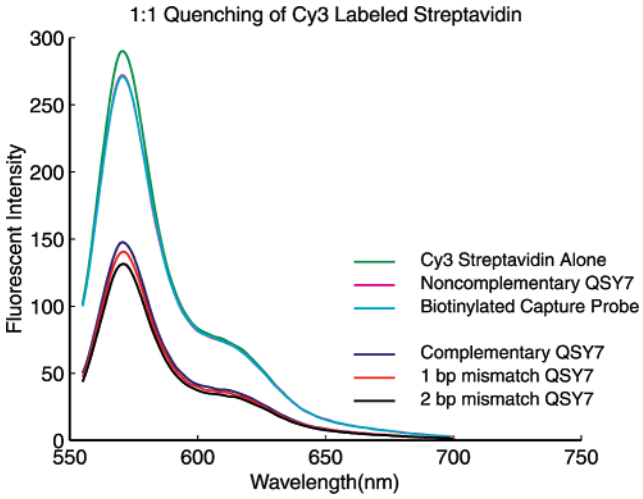

Figure 2. (Left) Steady-state quenching of DNA constructs. Neither addition of noncomplementary quencher nor biotinylated capture probe quenched the fluorescent protein. A reduction of roughly half of the fluorescence resulted from a 1:1 addition of biotinylated capture probe and complementary, singly, and doubly mismatched quencher probes.

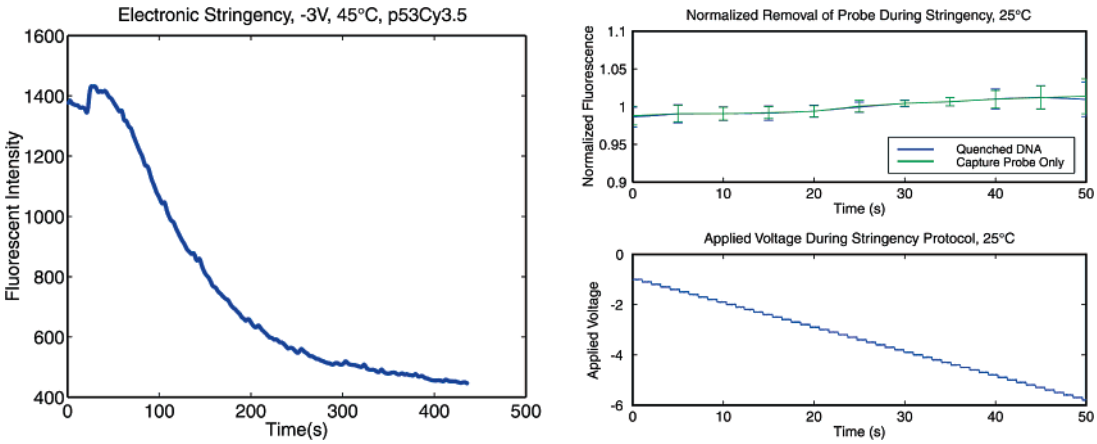

Figure 3. (Left) Electronic stringency at 45 °C for a complementary 19mer Cy3.5-labeled fluorescent probe. A majority of the bound probe is removed at −3 V at 45 °C. (Top Right) Normalized fluorescent response of surface-bound constructs during application of electronic stringency preconditioning. Note that, at room temperature, 25 °C, the voltages are below the dehybridization threshold, as no significant change in fluorescence is observed. (Bottom Right) Voltage used for preconditioning, −1 to −6 V, 25 °C. Background autofluorescence was measured at a value of 280 units.

Polyacrylamide-bound streptavidin DNA constructs were subjected to a sequence of 300 monophasic square wave oscillations at −3 V and −6 V at 10 Hz, with the lower gold electrode biased as the cathode. FRET constructs were analyzed under a custom-built epifluorescent microscope mounted on an air-stabilized optical table. Slides mounted atop a current-controlled Peltier stage set to 25 °C (LDT 5910B, ILX Lightwave, Bozeman, MT) were observed under a rotary Leica head fitted with long working distance objectives. Traces were recorded using an Orca-ER CCD camera (Hamamatsu C4742, Hamamatsu City, Japan), which achieved maximum frame rates of 104 Hz when connected to a National Instruments PCI-1422 board (National Instruments, Austin, TX). A 64 × 64 pixel subarray of the 12 bit camera field was set to 8 × 8 binning mode in order to provide maximal contrast.

Along with the complementary and mismatched DNA, controls included: unmodified acrylamide constructs, fluorescent streptavidin bound to the polyacrylamide, and fluorescent streptavidin bound to the acrylamide containing only a capture probe. Unmodified constructs with free Cy3-labeled DNA added to the 0.01X TBE buffer were also observed in order to control for fluorescent molecules migrating in and out of the focal plane. A set of five experiments were repeated for each type of DNA under each oscillatory influence.

Time series data were detrended by subtracting a 256th order zero-phase forward and reverse lowpass filter, normalized by 2 standard deviations and multiplied by a full-length, centered Hanning window prior to Fourier analysis. Normalized peak amplitudes were calculated as the mean and standard error of the maximum amplitude between 9 and 11 Hz, normalized by the sum of the data within each window.

We observed a sequence- and power-dependent oscillatory response across the FRET constructs. Figure 4 depicts a typical small signal output of a hinged transducer in response to −3 V, 5 Hz actuation. Harmonics of the square wave response were clearly visible in the Fourier spectrum.

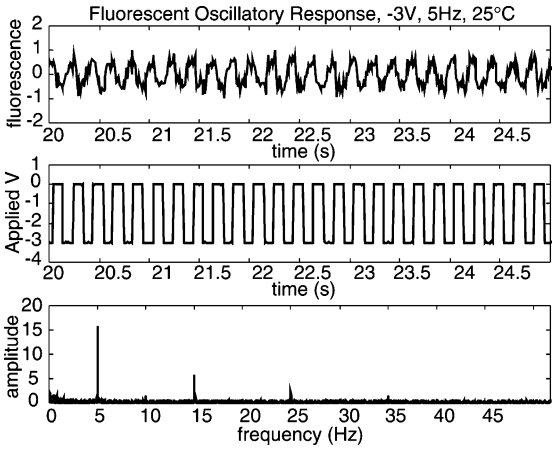

Figure 4. (Top) Driven transducer response. Raw fluorescence data was detrended by subtracting a lowpass filtered version of itself and then normalized by 2 standard deviations to recover small signal fluctuations. (Middle) The applied 5 Hz, −3 V voltage oscillation at room temperature. (Bottom) Absolute value of the discrete Fourier transform of the fluorescent signal.

As shown in Figure 5, 10 Hz, −3 V had little effect on the constructs at room temperature, but clear differences in amplitude were evident upon raising the voltage to −6 V. The data showed an increase in oscillatory response with complementarity. The matched system (Group 6) was significantly enhanced as compared to its level at lower power ($p < 0.034$, as calculated by a Student's t-test). None of the other groups showed a significant increase. The autofluorescent negative control (Group 2) did not tend to oscillate, indicating that fluctuations in autofluorescence were suppressed as compared to the FRET constructs. Likewise, free Cy3 in solution did not bring about discernible signals in the frequency domain.

Cy3−streptavidin (Group 7) exhibited relatively constant fluctuations in response to electrophoretic actuation. This positive control remained consistently high at each actuation mode, likely as a result of the environmental modulation of the quantum efficiency of the fluorophore.[24] The steady response of the fluorescent streptavidin was in clear contrast

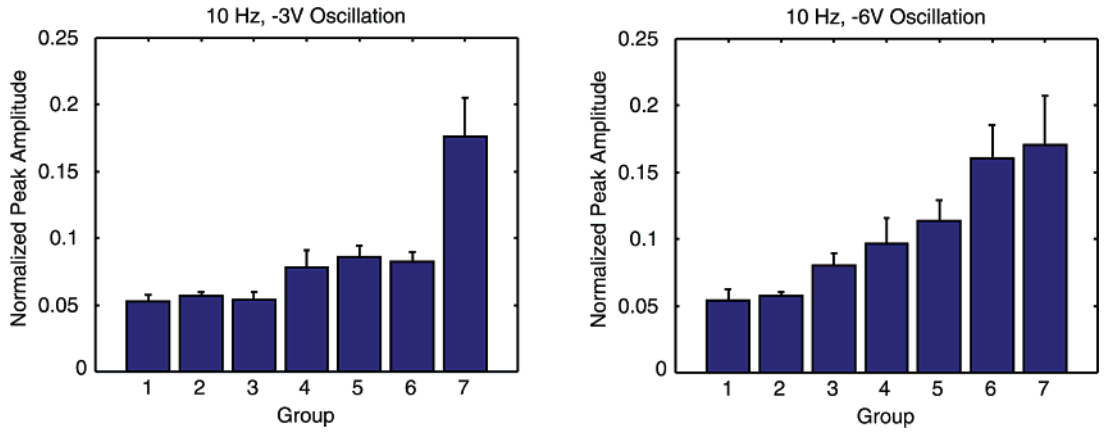

Figure 5. (Left) 10 Hz, −3 V oscillation. (Right) 10 Hz, −6 V oscillation. Group definitions: (1) free Cy3 DNA; (2) acrylamide constructs alone, negative control; (3) control; wild type p53 capture only; (4) one base pair mismatch; (5) two base pair mismatch; (6) complement; (7) Cy3−streptavidin alone, positive control. Complementary oscillations (Group 6) were significantly different at 10 Hz, −6 V than at 10 Hz, −3 V with a Student's unpaired t-test, $p < 0.034$.

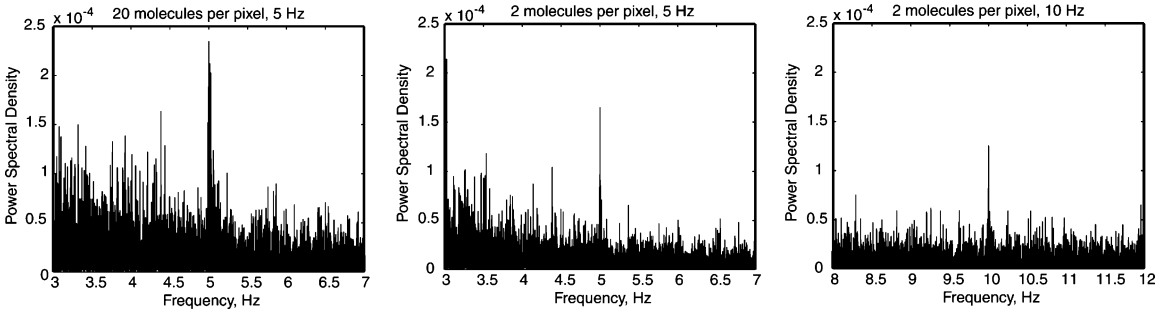

Figure 6. Power spectral densities for different concentrations of the electrophoretically actuated transduction mechanisms.

to the power-dependent oscillations of the fully assembled DNA system.

During actuation, it was also found that the capture strand control exhibited little oscillatory behavior, while the Cy3-labeled streptavidin responded strongly to the applied field. These findings were in contrast to passive quenching (Figure 2), where the capture strand did not influence the Cy3−streptavidin fluorescence. Given that the capture DNA is roughly 15 nm long, interactions between the single-stranded control and fluorescent streptavidin likely present a very different osmotic, electrostatic, and dynamic environment than the fluorescent streptavidin alone.

We found no correlation between normalized peak amplitude and power measured across a 470 Ω resistor in series with the gel constructs during the electronic stringency ramp, indicating that differences in oscillation amplitude were not attributed to inherent construct variations such as alternate low-resistance current paths in parallel with the FRET systems. Other random effects such as bubbles or electromechanically induced displacements within the constructs were uniformly distributed throughout the data and are unlikely to produce bias. Thus, the change in oscillatory responses are likely due to electrophoretic effects within the FRET system.

To test sensitivity gains resulting from the oscillatory behavior, serial dilutions of single base pair mismatch transduction systems were processed for electrophoretic actuation as described above. A −3 V to +1.4 V square wave at 5 or 10 Hz was applied to the gel constructs using an Agilent 33120A function generator for 30 min in order to accumulate the 2^{17} samples needed to facilitate a quality fast Fourier transformation of the data. The slight positive voltage was applied in order to help mitigate long-term pH shifts as a result of the electrolysis. Estimates of surface concentration assume that the FRET systems were bound uniformly across the gel construct, with areas calibrated against full- frame images of a well-characterized 80 μm diameter electrode, resulting in roughly 9 μm^2 per 8 × 8 binned pixel image. Spectra were calculated by taking the absolute value of the Fourier transform of the autocorrelation of the detrended, normalized time series. The center frequency of the data shown in Figure 6 was verified against spectral densities of the applied voltage.

Aliasing within the system prevented quantification of the long-term recordings, as the large datasets incurred memory caching within the software. However, it was evident that a concentration-dependent response of the actuated FRET system remained. Clear peaks in the frequency domain were visible down to near single-molecule levels, despite being roughly 5000 times lower than the autofluorescent background.

While it is premature to ascribe molecular mechanisms to explain the oscillatory differences between mismatched and matched behavior, power dependency indicates that a certain level of force is required before the differences in probe hybridization appear in response to electrophoretic actuation.

It can also be concluded that, on average, random fluctuations due to Brownian motion did not dominate the applied electrophoretic force within the FRET system.

Ideally, applied forces should provide enough leverage to unhinge the FRET pair without completely removing reporter probes from the target, as shown in Figure 1. Estimates of the force required for the initiation of DNA unzipping are widely varying in the literature (between 15 and 200 pN) and depend strongly on how fast the forces are applied.[25] The electronic stringency results shown in Figure 3 demonstrated that steady-state fields carried sufficient force to remove complementary oligonucleotide probes at higher temperatures. At lower temperatures, the constructs were more stable, remaining bound despite the application of the electric field.

Voltages were kept below the full dehybridization threshold in an attempt to prevent diffusional dynamics from blurring the results. The monophasic square wave actuation (between negative voltages and ground) further ensured that dehybridized probes were transported away from the bound constructs and could not diffuse back toward the constructs. Therefore, we conclude that the electrophoretic modulation of oligonucleotide probes resulted in sequence-dependent dynamics.

Future work on actuation will likely focus on increasing the frequency of modulation. It is known that phonon modes of DNA begin in the GHz range,[26,27] while transverse modes of long DNA segments have been observed using microwave absorption techniques.[28,29] Neither of these modes are amenable to FRET reporting, as fluorescent lifetimes are generally observed on the order of 1−10 ns.[30] However, hybridization kinetics of short hairpin loops have been measured in the 1−100 kHz range, well within the sampling rates available to a modulated fluorescent transduction system.[22,24]

It is not clear whether electrophoretic actuation will be able to attain sufficient field strengths to effect modulation of hybridization at these frequencies. At 25 °C, the mobility of a sodium ion is 5.19×10^{-4} cm^2/V·s.[31] A 10 V signal applied to electrodes spaced at 100 μm would enable a sodium ion to move roughly 50 nm at 100 kHz. While potentially sufficient to affect constructs located within the double layer, bulk modulation of nanoscale mechanisms seems unlikely at high frequencies using electrophoresis. However, the results shown here have interesting implications for externally actuated NEMS.

The design of the FRET constructs may also play a role in discerning the differences between complementary and mismatched probes. The proximity of the mismatch to the frayed end as well as interactions with surrounding base pairs may significantly affect the behavior of oscillatory systems. The lack of formalism surrounding the rates of prenucleated rehybridization makes it difficult to claim that all sequences will behave identically under electrophoretic perturbation. In particular, local free energy minima along the rehybridization isotherm could significantly affect the dynamics of certain sequences.[22] The probability of exploring secondary structures during rehybridization may also vary with the position and type of mismatch, in which case the relative magnitude of oscillatory response between complementary and mismatched sequences would be difficult to predict. Nevertheless, our interpretation that matched oscillations are greater than mismatched oscillations are consistent with earlier electrophoretic microarray data.[32]

In contrast to microarray formats where μm electrode spacing enables kV/m field densities to dehybridize oligonucleotides, the ability to modulate the hybridization of surface-bound constructs with a macroscopic counter-electrode suggests extension of this application to in situ hybridization methodologies, where paraffin-embedded tissue sections preclude the use of microarrays for electrophoretic actuation.

Acknowledgment. We thank Eugene Tu for his insight and discussions. Financial support from the NSF (DMI-0327077), von Liebig Center (2006-1), UCSD, and NIH Center of Excellence of Nanotechnology for Treatment, Understanding, and Monitoring of Cancer (U54 CA119335) is gratefully acknowledged.

References

(1) Szenajch, J.; Jasinski, B.; Kozak, A.; Kulik, J.; Chomicka, M.; Struzyna, J.; Nowecki, Z.; Rutkowski, P.; Ruka, W.; Kupsc, W.; Siedlecki, J.; Wiktor-Jedrzejczak, W. *Melanoma Res.* **2002**, *12*, 399−401.
(2) Champelovier, P.; Mongelard, F.; Seigneurin, D. *Anticancer Res.* **1999**, *19*, 2073−2078.
(3) Ghossein, R.; Bhattacharya, S. *Eur. J. Cancer* **2000**, *36*, 1681−1694.
(4) Ranieri, J. M.; Wagner, J. D.; Wiebke, E. A.; Azuaje, R.; Smith, M. L.; Wenck, S.; Daggy, J.; Coleman, J. J., III. *Plast. Reconstr. Surg.* **2005**, *115*, 1058−1063.
(5) Oldenburg, S. J.; Genick, C. C.; Clark, K. A.; Schultz, D. A. *Anal. Biochem.* **2002**, *309*, 109−116.
(6) Wang, J.; Liu, G.; Merkoci, A. *J. Am. Chem. Soc.* **2003**, *125*, 3214−3215.
(7) Authier, L.; Grossiord, C.; Brossier, P. *Anal. Chem.* **2001**, *73*, 4450−4456.
(8) Samama, B.; Plas-Roser, S.; Schaeffer, C.; Chateau, D.; Fabre, M.; Boehm, N. *J. Histochem. Cytochem.* **2002**, *50*, 1417−1420.
(9) Cao, Y. C.; Jin, R.; Mirkin, C. A. *Science* **2002**, *297*, 1536−1540.
(10) Taton, T. A.; Mirkin, C. A.; Letsinger, R. L. *Science* **2000**, *289*, 1757−1760.
(11) Epstein, J. R.; Lee, M.; Walt, D. R. *Anal. Chem.* **2002**, *74*, 1836−1840.
(12) Lin, L.; Zhao, H.; Li, J.; Tang, J.; Duan, M.; Jiang, L. *Biochem. Biophys. Res. Commun.* **2000**, *274*, 817−820.
(13) Su, M.; Li, S.; Dravid, V. *Appl. Phys. Lett.* **2003**, *82*, 3562−3564.
(14) Gaylord, B. S.; Heeger, A. J.; Bazan, G. C. *Proc. Natl. Acad. Sci. U.S.A.* **2002**, *99*, 10954−10957.
(15) Dill, K.; Montgomery, D.; Ghindilis, A.; Schwarzkopf, K. *J. Biochem. Biophys. Methods* **2004**, *59*, 181−187.
(16) Kim, E.; Kim, K.; Yang, H.; Kim, Y. T.; Kwak, J. *Anal. Chem.* **2003**, *75*, 5665−5672.
(17) Santangelo, P. J.; Nix, B.; Tsourkas, A.; Bao, G. *Nucleic Acids Res.* **2004**, *32*, e57.
(18) Bentzen, E. L.; Tomlinson, I. D.; Mason, J.; Gresch, P.; Warnement, M. R.; Wright, D.; Sanders-Bush, E.; Blakely, R.; Rosenthal, S. J. *Bioconjugate Chem.* **2005**, *16*, 1488−1494.
(19) Bhanot, G.; Louzoun, Y.; Zhu, J.; DeLisi, C. *Biophys. J.* **2003**, *84*, 124−135.
(20) Heller, M. J.; Tu, A. T.; Maciel, G. E. *Biochemistry* **1974**, *13*, 1623−1631.
(21) Chen, C.; Russu, I. M. *Biophys. J.* **2004**, *87*, 2545−2551.
(22) Ansari, A.; Kuznetsov, S. V.; Shen, Y. *Proc. Natl. Acad. Sci. U.S.A.* **2001**, *98*, 7771−7776.
(23) Ansari, A.; Shen, Y.; Kuznetsov, S. V. *Phys. Rev. Lett.* **2002**, *88*, 069801.
(24) Braun, D.; Libchaber, A. *Appl. Phys. Lett.* **2003**, *83*, 5554−5556.

(25) Cocco, S.; Monasson, R.; Marko, J. F. *Phys. Rev. E* **2002**, *65*, 041907.
(26) Woolard, D. L.; Globus, T. R.; Gelmont, B. L.; Bykhovskaia, M.; Samuels, A. C.; Cookmeyer, D.; Hesler, J. L.; Crowe, T. W.; Jensen, J. O.; Jensen, J. L.; Loerop, W. R. *Phys. Rev. E* **2002**, *65*, 051903.
(27) Prohofsky, E. W. *Bioelectromagnetics* **2004**, *25*, 441−451.
(28) Edwards, G. S.; Davis, C. C.; Saffer, J. D.; Swicord, M. L. *Biophys. J.* **1985**, *47*, 799−807.
(29) Van, Zandt, L. L. *Phys. Rev. Lett.* **1986**, *57*, 2085−2087.
(30) Krishnan, R.; Saitoh, H.; Terada, H.; Centonze, V.; Herman, B. *Rev. Sci. Instrym.* **2003**, *7*, 2714−2721.
(31) Grodzinsky, A.; Eisenberg, S. *Fields Forces and Flows in Biological Tissues and Membranes.* Departments of Electrical Engineering and Computer Science, Mechanical Engineering, and Harvard-MIT Division of Health Sciences Technology, Department of Biomedical Engineering, Boston University: Boston, 1995.
(32) Heller, M. J.; Tu, E.; Sosnowski, R. G.; O'Connell, J. P.; U.S. Patent 6,048,690, April 11, 2000.

NL063014X